On the effects of numerical integration on accuracy of microplane modeling of shape memory alloys

A. Jalalpour[a], M. Kadkhodaei[b], S. Arbab-chirani[c], M. Lakrit[d], M. Barati[e], L. Pino[f], L. Saint-Sulpice[g], S. Calloch[h]

a. Department of Mechanical Engineering, Isfahan University of Technology, Isfahan 84156-83111, Iran. Email: a.jalalpour.mech@gmail.com

b. Department of Mechanical Engineering, Isfahan University of Technology, Isfahan 84156-83111, Iran. Email: kadkhodaei@cc.iut.ac.ir

c. ENIB, UMR CNRS 6027, IRDL, F-29200 Brest, France. Email: arbab@enib.fr

d. ENSTA Bretagne, UMR CNRS 6027, IRDL, F-29200 Brest, France. Email: mohamed.lakrit@ensta-bretagne.fr

e. ENIB, UMR CNRS 6027, IRDL, F-29200 Brest, France. Email: barati@enib.fr

f. ENIB, UMR CNRS 6027, IRDL, F-29200 Brest, France. Email: pino@enib.fr

g. ENIB, UMR CNRS 6027, IRDL, F-29200 Brest, France. Email: sulpice@enib.fr

h. ENSTA Bretagne, UMR CNRS 6027, IRDL, F-29200 Brest, France. Email: sylvain.calloch@ensta-bretagne.fr

Abstract:

In this paper, predictions of the so-called Microplane model for shape memory alloys (SMAs) and the effect of different numerical schemes under various proportional and nonproportional loadings are investigated. Accordingly, numeric schemes with central symmetry are shown to possess shortcomings in addressing tension-torsion coupling in the response of SMAs. Therefore, an enhanced numeric scheme is proposed in order to add tension-torsion coupling to a formerly-developed microplane model of Shape memory alloys. The presented integration scheme gives rise to numerical results which are in acceptable agreements with experimental findings in both 1-D and 3-D cases.

Key words: Shape Memory Alloys, Microplane theory, Proportional and nonproportional loadings, tension-torsion coupling

1 Introduction

SMAs have thermo-mechanical behaviors which produce two distinguished characteristics known as Shape Memory Effect (SME), recovering a large deformation caused by mechanical stresses upon heating up to a specific temperature due to the transformation of detwinned martensite to austenite, and Pseudoelasticity (PE), the appearance of no residual strain after an inelastic loading/unloading cycle at high enough temperatures. These features create a vast range of applications for these alloys such as biomedical engineering, aerospace industries, mechanical engineering, and robotics. These applications require a constitutive model to predict materials behaviors under complex loadings.

Considering transitions between austenite and martensite phases in these materials and the martensite volume fraction as an internal variable for SMAs, Tanaka [1] provided a 1-D constitutive model, later modified by Liang and Rogers [2], to predict pseudoelastic response. Brinson [3] proposed to separate twinned and detwinned parts of the martensite volume fraction as internal variables in 1-D models so that such a model is able to predict SME as well. The first 3-D constitutive model was developed by Boyd and Lagoudas [4] by generalizing 1-D constitutive models to 3-D cases. But, in a general 3-D loading, reorientation i.e. variations in the configuration of the martensite lattice and phase transformation may occur simultaneously. Lim and McDowell [5] showed that the transformation strain rate vector and the deviatoric stress vector are not parallel in nonproportional loadings; therefore, any 3-D model based on the J_2 or J_2–J_3 plasticity for the transformation strain rate is limited to proportional loadings. Peng et al. [6] generalized the definition of effective stress to model SMAs under nonproportional loadings using normality rule. A phenomenological model was developed by Bouvet et al. [7] for modeling PE in which the transformation strain was calculated by a potential function.

Microplane theory is an approach for 3-D constitutive modeling, based on a 1-D constitutive model, with the ability of predicting reorientation under nonproportional loadings [8,9,10]. In this theory, at any material point, a 1-D law is applied for the related stress and strain acting on any plane which passes through that point. This process is accomplished via numerical integration over a unit sphere. To calculate integrals over a hemisphere at each integration point, Bazant et al. [11] suggested a 21-point numerical scheme which has been vastly utilized in microplane modeling of SMAs. The first microplane-based model was proposed by Brocca et al. [12] by the projection of the stress vector on each plane. The shear stress on each plane was separated into the two random vectors, and the martensite volume fraction was calculated by these shear vectors from the same phase diagram. Kadkhodaei et al. [10] proposed to use a unique shear vector projected from the stress traction on each plane. Using the volumetric–deviatoric split, they showed that the microplane theory can predict reorientation under nonproportional loadings.

The integration over a unit sphere is used in many fields including meteorology, chemistry, and physics. The numerical scheme proposed by Bazant et al. [11] is based on the Gauss integration on a semi-sphere due to the symmetry of stress tensor, and 21-point integration was shown to give the most precise results for modeling SMAs. High-order Gauss scheme was proposed by Delley [13] in which the unit sphere is divided to the Tetrahedrons. Heo et al. [14] suggested symmetric cubature formulae with 13 to 39 points on the surface of the unit sphere. Hannay et al. [15] presented the Fibonacci numerical integration in which the angular distance between the nodes on the surface is based on the Fibonacci sequence. According to the location of electrons on the surface of a sphere for the minimum electrical charge, Fliege et al. [16] proposed a numerical scheme with equal-distance distribution of the nodes on the surface of a unit sphere. Due to the physical aspect of this scheme, it is allowed to rotate the nodes on the surface. Comparing exact integration of some basic functions with this numerical scheme, they showed that a scheme with more nodes does not guarantee more precision. Eheret et al. [17] studied a class of constitutive models based on integration on a unit sphere. They showed that the integration schemes can affect the material isotropy and cause directional bias in the material behavior. They classified the numerical schemes into with- and without-central symmetric. Huang et al. [18] studied effects of numerical schemes, proposed by Bazant, of the microplane constitutive models (M4) for concrete.

Mehrabi et al. [19] conducted tension-torsion experiments on thin-walled SMAs samples and observed axial strains in pure torsion test which indicates the so-called tension-torsion coupling. Microplane models founded on 21-point integration cannot predict the tension-torsion coupling. Using the generalized effective stress and strain associated with microplane theory, they presented a model for predicting tension-torsion behavior.

In the present work, this issue is addressed and different numerical schemes in calculating the microplane integrals are evaluated to propose an approach using which microplane formulations will be able to predict tension-torsion coupling.

2 Introduction to Microplane Formulation

As mentioned, SMAs have thermo-mechanical behaviors and their phase would change under different stress-temperature conditions. Fig.1 shows the stress-temperature phase diagram in which the different SMAs' phases are presented and is used to calculate the evolution of the martensite volume fraction [3]. Due to the different properties of the austenite and martensite, material parameters such as young modulus can be evaluated as following in which E_A and E_M represent austenite and martensite's young modulus, respectively. For some SMA materials a general 4-line phase diagram, as shown in Fig. 2, has a better agreement.

$$E(\xi) = (1-\xi)E_A + \xi E_M$$

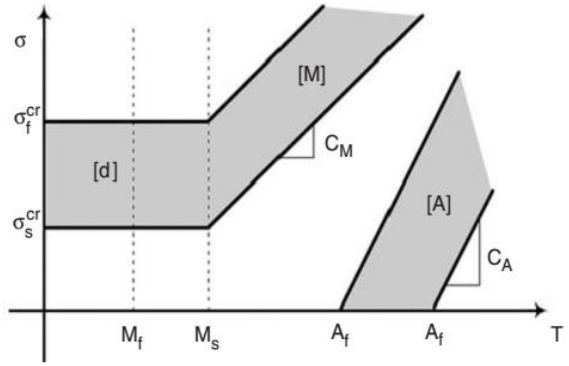

Fig. 1. Stress-temperature phase diagram

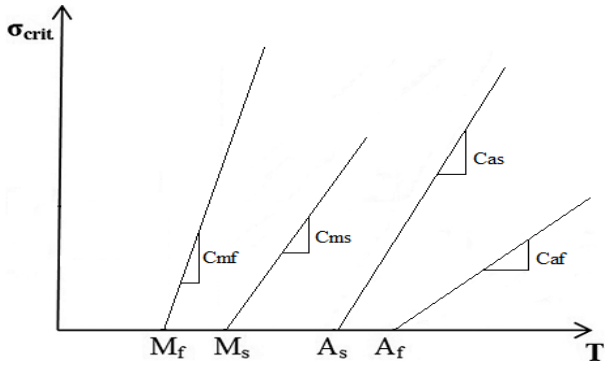

Fig. 2. Phase diagram for evaluating martensite volume fraction

A 3-D macroscopic constitutive model for SMAs based on microplane theory is explained in this section. Based on Fig. 3, the normal and tangent stress vector due to the stress tensor's projection are [10]:

$$\sigma_N = N_{ij}\sigma_{ij},\ N_{ij} = n_i n_j,\ t_i = \frac{\sigma_{ik}n_k - \sigma_N n_i}{\sqrt{\sigma_{rs}\sigma_{rt}n_s n_t}}$$

$$\sigma_T = T_{ij}\sigma_{ij},\ T_{ij} = \frac{1}{2}(t_i n_j + t_j n_i)$$

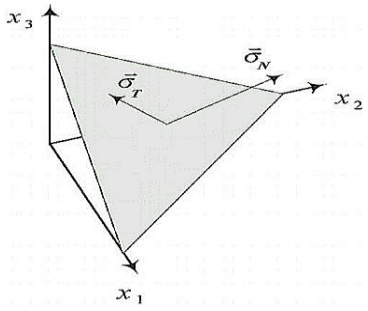

Fig. 3. Stress traction decomposition on microplanes

where σ_N, σ_T and n represent normal stress, shear stress and unit normal vector on each microplane, respectively. In the homogenization process, using the principle of complementary virtual, the macroscopic strain is [10]:

$$\int_\Omega \varepsilon_{ij}\delta\sigma_{ij}d\Omega = \int_\Omega (\varepsilon_N \delta\sigma_N + \varepsilon_T \delta\sigma_T)d\Omega$$

in which Ω is the surface of a unit sphere representing all possible microplane orientations passing through a material point. The linear elastic relation for normal stress and strain is assumed. As the phase transformation is due to the shear deformation, the total inelastic strain is considered to be only from

shear strains on the microplanes. Splitting elastic and transformation strains, once can obtain the following relations:

$$\varepsilon_{ij}=\varepsilon_{ij}^{e}+\varepsilon_{ij}^{tr},\quad \varepsilon_{ij}^{e}=-\frac{\nu}{E(\xi)}\sigma_{ss}\delta_{ij}+\frac{3}{4\pi}\frac{1+\nu}{E(\xi)}\sigma_{rs}\int_{\Omega}(N_{ij}N_{rs}+T_{ij}T_{rs})d\Omega,\quad \varepsilon_{ij}^{tr}=\frac{3}{4\pi}\varepsilon^{*}\xi_{s}(\bar{\sigma},T)\int_{\Omega}T_{ij}d\Omega$$

where ξ and ξ_s are the martensite and stress-induced martensite volume fraction and $\bar{\sigma}$ is the von Mises effective stress and ϵ^* is recoverable strain. Application of 21-point numerical scheme for calculating the integrals gives:

$$\varepsilon_{ij}^{e}=-\frac{\nu}{E(\xi)}\sigma_{kk}\delta_{ij}+\frac{6(1+\nu)}{E(\xi)}\sigma_{rs}\sum_{q=1}^{21}W(q)(N_{ij}(q)N_{rs}(q)+T_{ij}(q)T_{rs}(q)),\quad \varepsilon_{ij}^{t}=6\varepsilon^{*}\xi_{s}\sum_{q=1}^{21}W(q)T_{ij}(q)$$

in which W is the weight of each plane and the index q refers to each individual plane. Due to the symmetry of the 21-point method, these 21 points are on the surface of a unit hemisphere [10].

3 Numerical Investigations

In this section, the response of an SMA with the material properties presented in table 1 under nonproportional loadings using 21-point numerical integration is investigated. In the first case, a uniaxial stress is applied to the amount of 500 MPa in x direction; then, this stress is held constant while stress in the y direction is simultaneously increased up to 500 MPa. After the magnitude of the stress reaches the desired level, the stress in x direction will reduce to zero while the stress in y direction is constant. The temperature is assumed to be 50^0C in all cases. At the end, the stress in the y direction will diminish. In Fig. 4, results of this tension-tension nonproportional loading cycle are shown.

Table 1. Material Parameters in figures 4 to 6

E_A $[GPa]$	E_M $[GPa]$	M_f [°C]	M_s [°C]	A_s [°C]	A_f [°C]	C_M $[\frac{MPa}{°C}]$	C_A $[\frac{MPa}{°C}]$	σ_s^{cr} $[MPa]$	σ_f^{cr} $[MPa]$	ε^*
67	26.3	9	18.4	34.5	49	8	13.8	100	170	0.067

As it is presented in Fig. 4, at the first stage, the axial strain in x direction increases while the axial strain in y direction also increases in the negative direction due to the lateral effect. In the second stage, based on the transformation stress at the end of the previous step, the transformation is completed so the relation of the axial strains would not be linear owing to the reorientation of the martensite variants. Moreover, there is a jump at the beginning caused by the numerical integration algorithm and change in the status of the stress from the uniaxial to the biaxial condition. In a uniaxial situation, traction on some planes is zero; but, when stress in the second direction is applied, these planes would have traction on them and they would affect on the resulted strain tensor. In this stage, the strain in y direction would increase in the positive magnitude. Stage 3 is similar to step 2 except in this step the stress is being removed in x direction. At the beginning of the forth step, there would be again a jump like the one at the end of the first stage because of the same reason which is change in the stress state from biaxial to the uniaxial loading.

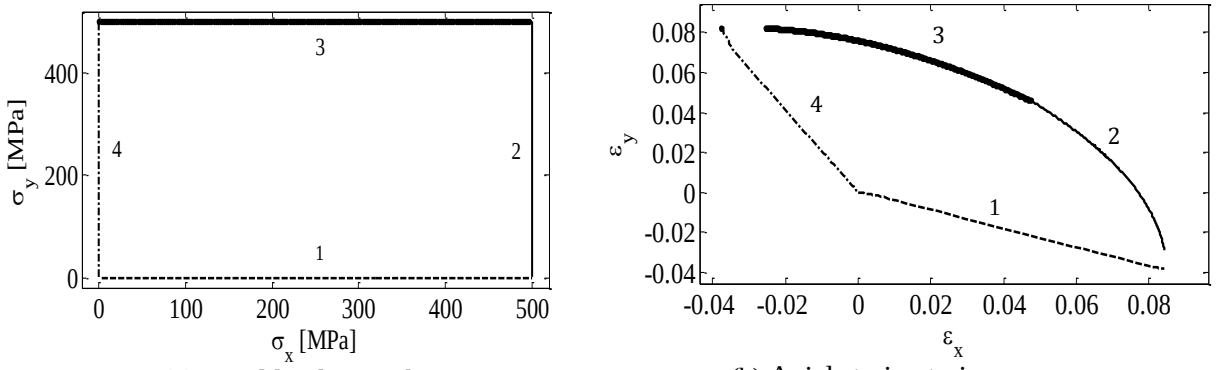

(a) Axial loading path (b) Axial strain-strain response

Fig. 4. Details of tension-tension nonproportional loading using 21 -point integration scheme

Fig. 5 shows another case in which the uniaxial stress increases up to 500 MPa; then, the axial stress is held constant and the shear stress is applied up to the amount of 500MPa. In the next stage, the axial stress is removed while the shear stress is constant. Finally, at the last step, the remaining shear stress would decline. At the end of the first step, the transformation is complete and the material is elastic detwinned martensite. At the beginning of the second stage, the shear strain have a jump resulted from the same reason in the tension-tension case. In the second and third steps, the microplane theory reveals

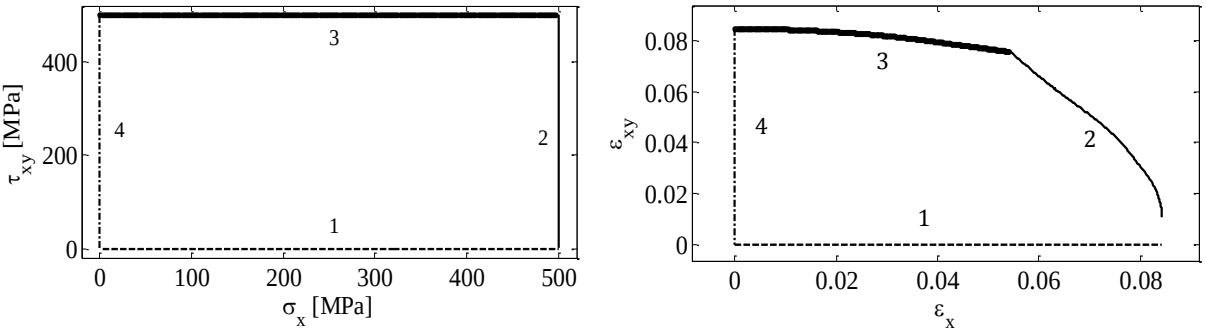

(a) Stress path (b) Axial-Shear strain response

Fig. 5. Details of tension-torsion nonproportional loading using 21 -point integration scheme

reorientation due to change in the direction of the principal axes of the stress tensor so the martensite variants would alter their orientation as well. At the last step, as it is shown in Fig. 5, axial strain is zero when there is only shear stress which means inability of the simulation to predict tension-torsion coupling using 21-point numerical integration.

Owing to the special arrangement of the microplanes, symmetric planes cancel out their values. These values for Bazant's 21-point numerical scheme for simple shear are presented in table 2. As is shown, $\sum_{q=1}^{21} W(q) T_{11}(q)$ and hence ϵ_{11} would be eliminated. Therefore, centrosymmetric numerical methods cannot predict the expected tension-torsion coupling.

Table 2. T_{11} and weight of each plane in 21-point numerical scheme in simple shear loading

# of planes	1	2	3	4	5	6	7	8	9	10
T_{11}	0	0.24	-0.24	-0.183	0	0.183	-0.108	0.108	0	-0.459
W	0.0198	0.0198	0.0198	0.0198	0.0198	0.0198	0.0254	0.0254	0.0254	0.0254
# of planes	11	12	13	14	15	16	17	18	19	20	21
T_{11}	0.27	-0.27	0.458	-0.192	0.192	-0.321	0	0.321	0	0	0
W	0.0254	0.0254	0.0254	0.0254	0.0254	0.0254	0.0254	0.0254	0.0254	0.0254	0.0254

Consequently, a non-centrosymmetric numerical scheme needs to be applied to take account of the tension-torsion coupling. After evaluating different non-centrosymmetric numerical schemes, the 25-point numeric scheme proposed by Fliege et al. (1999) showed a reasonable axial strain during pure shear loading which is expected as is presented in Fig. 6.

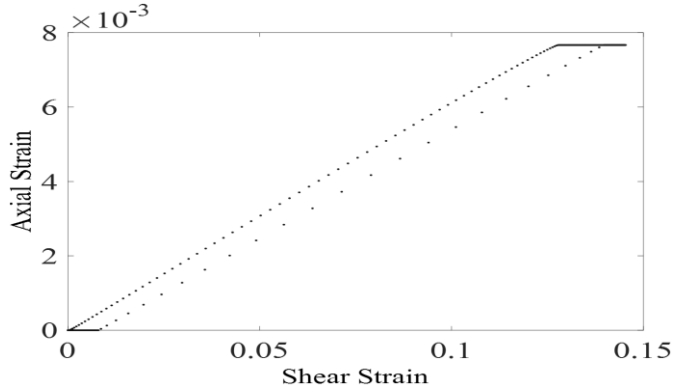

Fig. 6. Axial strain in pure shear loading when 25-point integration is applied.

4 Experimental Validation

Results of the microplane model, using the 25-point numerical integration, are compared with experimental findings in proportional and nonproportional tests. The material parameters are obtained from axial and simple shear tests, according to Fig. 7, and are presented in table 2.

$$\sigma_{eq} = \sqrt{\sigma^2 + C_s^2 \tau^2}\,, \qquad \varepsilon_{eq} = \sqrt{\varepsilon^2 + \frac{\gamma^2}{C_E^2}}\,, \qquad k_s = \frac{C_s}{\sqrt{3}} = \frac{\sigma_0^s}{\sqrt{3}\tau_0^t}\,, \qquad k_E = \frac{\sqrt{3}}{C_E} = \frac{\sqrt{3}\varepsilon_0^s}{\gamma_0^t}$$

The coefficients k_S and k_E state the extent of coupling between tension and torsion and are called effective stress coefficient and effective strain coefficient, respectively, to match the 1-D experiment and the microplane results. The coefficient of k_S is determined by the yield stresses in uniaxial tension,σ_0^s, and in pure torsion, τ_0^t, and coefficient of k_E is defined by the axial strain corresponding to the yield stress in pure tension, ε_0^t, and the yield shear strain in pure torsion, γ_0^t [20].
Using 4-line phase diagram, as is shown in Fig. 2, the martensite volume fraction can be evaluated.

Table 2. Material parameters in figures 7 to 10

E_A $[GPa]$	E_M $[GPa]$	M_f [℃]	M_s [℃]	A_s [℃]	A_f [℃]	C_{MS} $[\frac{MPa}{℃}]$	C_{MF} $[\frac{MPa}{℃}]$	C_{AS} $[\frac{MPa}{℃}]$	C_{AF} $[\frac{MPa}{℃}]$
61.943	34.65	-114	-107	-99.14	-88.17	2.41	4.63	3.16	2.02
ε^*	ν	C_s	C_E						
0.0253	0.3	1.495	1.495						

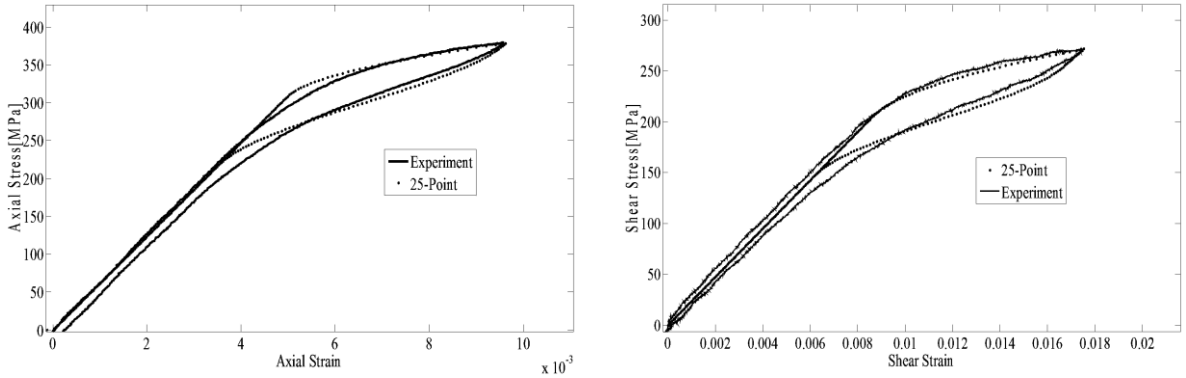

(a) (b)

Fig. 7. The utilized axial and shear tests to obtain material parameters for 25-point integration

The results of three unproportional loading cases with different paths are compared with the use of 21-point and 25-point numerical schemes. As is shown in Fig. 8, comparison of the results reveal that the 25-point scheme leads to a better agreement with the experimental observations. It is obvious that the 25-scheme shows axial strain at the end of the second step while the stress state is pure shear.

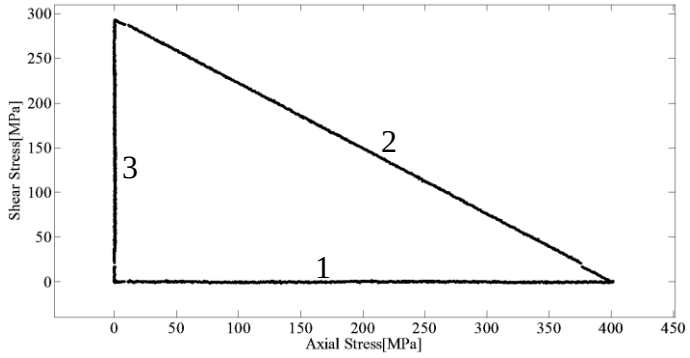

(a)

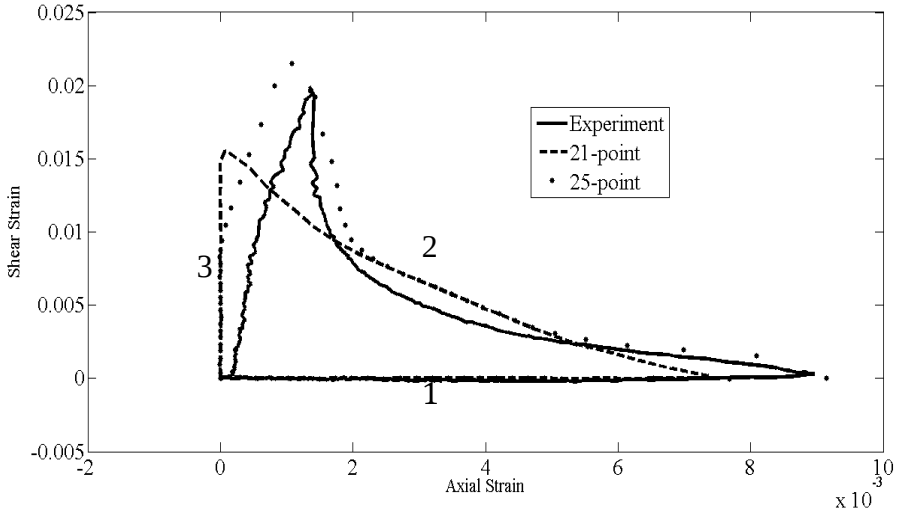

(b)

Fig. 8. Nonproportional tension-torsion results, case(1)

In Fig. 8(a), at the end of the second step, only shear stress is applied and, as Fig. 8(b) shows, at this point, there is axial strain beside the shear strain which is predicted only by 25-point scheme. Based on Fig. 9(b) and 10(b), the 25-point scheme can predict the experimental results more closely compared with the 21-point scheme. The maximum difference between the 25-point scheme and the experiment results are 18.5% and 15.2%for case (2) and case (3), respectively.

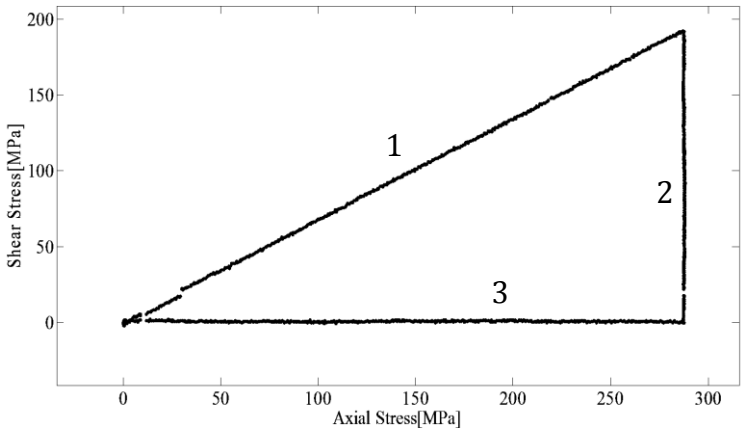

(a)

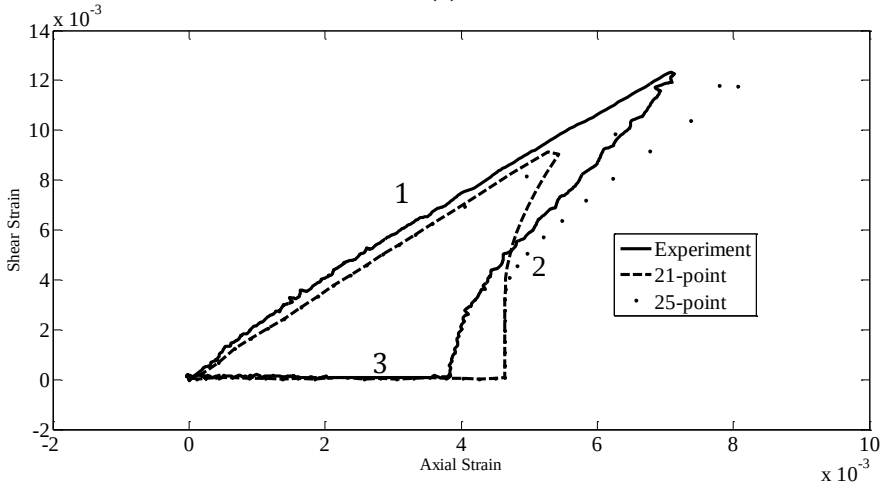

(b)

Fig. 9. Nonproportional tension-torsion results, case (2)

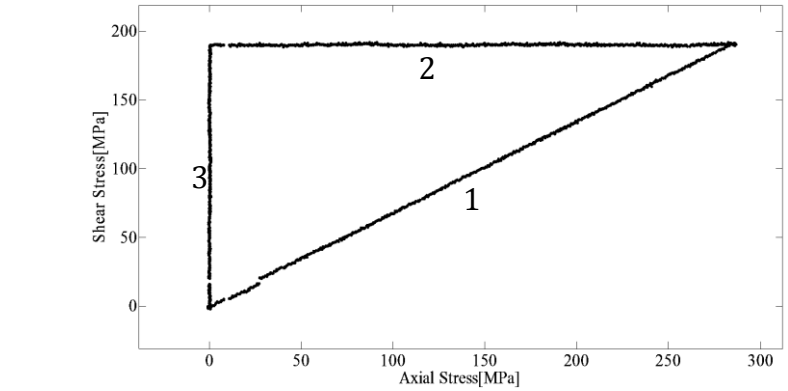

(a)

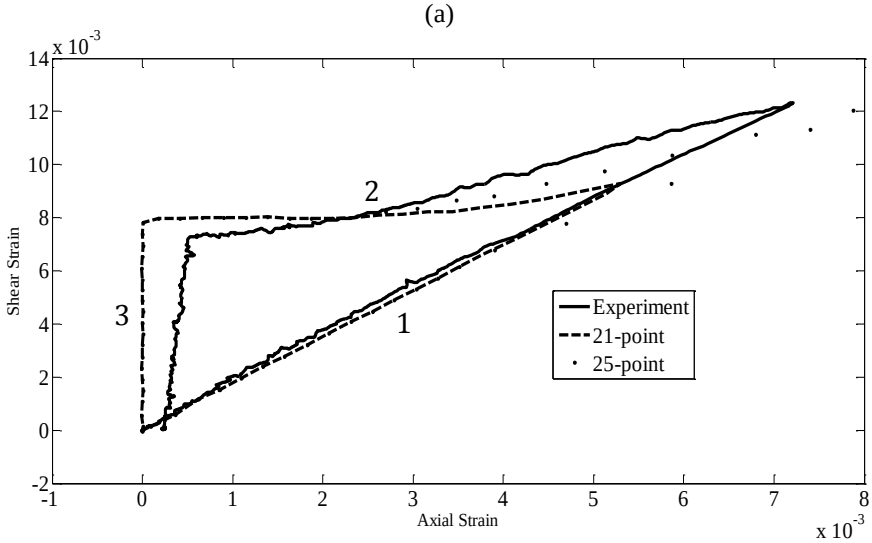

(b)

Fig. 10. Nonproportional tension-torsion results, case (3)

Conclusion

In this study, the 21-point integration scheme in microplae modeling of SMAs was studied. It was shown that this method can result in some discontinues responses in the case of nonproportional loadings. In fact, because of the centrosymmetry instinct of this scheme, it is not possible to reach the coupling between tension and torsion. Although the developed 25-point numeric scheme may possess sort of the same discontinuity, thanks to its non-centrosymmetry, it enables the microplane formulation to predict tension-torsion coupling under nonproportional loadings.

References

[1] K. Tanaka, S. Kobayashi and Y.Sato, Thermomechanics of Transformation Pseudoelasticity and Shape Memory Effect in Alloys, International Journal of Plasticity, vol. 2, pp. 59-72, 1986.

[2] C. Liang and C. A. Rogers, One-Dimensional Thermomechanical Constitutive Relations for Shape Memory Materials, Journal of Intelligent Material Systems and Structure, 1990.

[3] L. C. Brinson, One-Dimensional Constitutive Behavior of Shape Memory Alloys: Thermomechanical Derivation with Non-Constant Materials Functions and Redefined Martensite Internal Variable, Intelligent Material System and Structures, vol. 4, pp. 229-242, 1993.

[4] Boyd, J.G. and Lagoudas, D.C. (1994), Thermomechanical Response of Shape Memory Composites, Journal of Intelligent Materials Systems and Structures, 5:333–346.

[5] T. J. Lim, D. L. McDowell, Mechanical Behavior of a Ni-Ti Shape Memory Alloy under Axial-Torsional Proportional and Nonproportional Loading, Journal of Engineering Materials and Technology, 1999.
[6] X. peng, Y. yang, S. huang, A comprehensive description for shape memory alloys with a two-phase constitutive model, International Journal of Solids and Structures, 2000.
[7] C. Bouvet, S. Calloch, C. Lexcellent, A phenomenological model for Pseudoelasticity of shape memory alloys under multiaxial proportional and Nonproportional loadings, European Journal of Mechanics, 2003.
[8] Kadkhodaei, M., Salimi, M., Rajapakse, R. K. N. D., & Mahzoon, M. ,Microplane modelling of shape memory alloys, Physica Scripta, 2007(T129), 329.
[9] Mehrabi, R., & Kadkhodaei, M., 3D phenomenological constitutive modeling of shape memory alloys based on microplane theory, Smart Materials and Structures, 22(2), 025017, 2013.
[10] Mehrabi, R., Kadkhodaei, M., & Chirani, S. A., Microplane modeling of martensite reorientation in shape memory alloys, ECCOMAS, 2012.
[11] Bažant, Z. P., OR, B. H., Efficient numerical Integration on the Surface of a Sphere, ZAMM. Z. angew. Math. u. Mech, pp. 37-40, 1986.
[12] M. brocca, L. C. Brinson, Z. P. Bazant, three-dimensional constitutive model for shape memory alloys based on microplane model, Journal of the Mechanics and Physics of solids, 2001.
[13] B. Deley, High order Integration Schemes on the Unit Sphere, Journal of Computational Chemistry, vol. 17, no. 9, 1996.
[14] S. Heo and Y. Xu, Constructing fully symmetric cubature formulae for the sphere, Mathematics of Computation, vol. 70, pp. 269-279, 2000.
[15] J H Hannay and J F Nye, Fibonacci numerical integration on a sphere, Journal of Physics A: Mathematical and General, pp. 11591-11601, 2004.
[16] Jorg Fliege and Ulrike Maier, The distribution of points on the sphere and corresponding cubature formulae, IMA Journal of Numerical Analysis, vol. 19, pp. 317-334, 1999.
[17] A. E. Ehret,M.Itskov and H.Schmid, Numerical integration on the sphere and its effect on the material symmetry of constitutive equations-A comparative study, Int. J. Numer. Meth. Engng, vol. 81, no. Wiley InterScience, pp. 189-206, 2010.
[18] L. C. Huang, J. Li, N. V. Tue, J. Nemecek, T. Püschel, Numerical aspects of microplane constitutive models for concrete, Applied Mathematical Modelling 41 (2017) 530–548.
[19] R. Mehrabi, M. T. Andani, M. Kadkhodaei, M. Elahinia, Experimental Study of NiTi Thin-Walled Tubes under Uniaxial Tension, Torsion, Proportional and Non-Proportional Loadings, Experimental Mechanics, 2015.
[20]R. Mehrabi, M.T. Andani, M. Elahinia, M. Kadkhodaei, "Anisotropic behavior of superelastic NiTi shape memory alloys; an experimental investigation and constitutive modeling," *Mechanics of Materials,* 2014.